ISSN 0036-0236, Russian Journal of Inorganic Chemistry, 2020, Vol. 65, No. 9, pp. 1326–1332. © Pleiades Publishing, Ltd., 2020.

SYNTHESIS AND PROPERTIES OF INORGANIC COMPOUNDS

Alkalinity Effect on Characteristic Properties and Morphology of Magnesium Phosphate Hydrates

F. T. Senberber[a], * and E. Moroydor Derun[b]

[a] *Department of Civil Engineering, Nisantasi University, Istanbul, 34375 Turkey*

[b] *Department of Chemical Engineering, Yildiz Technical University, Istanbul, 34349 Turkey*

**e-mail: fatma.senberber@nisantasi.edu.tr*

Received February 4, 2020; revised March 24, 2020; accepted April 20, 2020

Abstract—Magnesium oxide (MgO) and orthophosphoric acid (H_3PO_4) have been reacted at different pH values to study the effects of alkalinity on the characteristic features of magnesium phosphate material. The phases of the synthesized samples have been identified as newberyite (with the chemical formula of $MgHPO_4 \cdot 3H_2O$ and the pdf no. 01-075-1714) and magnesium phosphate hydrate (with the chemical formula of $Mg_3(PO_4)_2 \cdot 22H_2O$ and the pdf no. 00-044-0775), in the X-ray powder diffraction analyses results. The characteristic band values of samples have been characterized by FTIR and Raman spectroscopies. The differences in morphologies have been studied with Scanning Electron Microscope (SEM). The largest particles in the range of 3.16–9.85 μm have been seen in the shape of nested flat sheets at pH 10 while the smallest particles between 1.17–2.04 μm have been obtained in the shape of an ellipse at pH 7. According to the thermogravimetric analyses, the differences in thermal behaviours have been determined. $MgHPO_4 \cdot 3H_2O$ has lost its crystal water by a two-step reaction while $Mg_3(PO_4)_2 \cdot 22H_2O$ has dehydrated by a single-step reaction. Obtained results indicate that the crystal structure and surface morphology of the synthesized compound can be modified by the alkalinity of the reaction medium.

Keywords: hydrothermal synthesis, magnesium phosphate, morphology, thermal behaviour, pH

DOI: 10.1134/S0036023620090156

INTRODUCTION

Magnesium phosphate is a member of metal phosphate family which includes the elements of magnesium, phosphorus, oxygen and hydrogen. That type of phosphate has features of the chemical resistance, heat resistance and water insolubility [1, 2]. The advantage of these materials is that they contain a combination of environmentally friendly harmless elements. They are generally used as the anticorrosive inorganic pigments [3–5]. They specifically preferred as the catalysts in the organic transformation reactions such as dehydration of 2-propanol, the oxidative dehydrogenation of ethane and the oxidative transformation of methane [2, 6, 7]. Different phosphate compounds were also used in food preservatives, ceramics, water treatment, metallurgy, dental applications and nuclear systems. The addition of the magnesium phosphate compounds to cement compositions requires some advantages, such as small drying shrinkage, very rapid setting and hardening, good bonding strength, high early strength, high wear resistance, hardening at low temperature and excellent frost resistance [8, 9]. There are different types of magnesium phosphates such as hydrophosphates ($MgHPO_4 \cdot 3H_2O$, $Mg_3PO_4 \cdot 5H_2O$, $Mg_3PO_4 \cdot 8H_2O$, $Mg_3PO_4 \cdot 5H_2O$, $Mg_3PO_4 \cdot 22H_2O$ or $Mg_2PO_4OH \cdot 4H_2O$) and chemically bonded phosphate ceramics ($Mg_3(PO_4)_2$ and $Mg_2P_2O_7$) [3–21].

The first studies about phosphate ceramics indicated that hydrophosphates can be prepared by using the reaction of various inorganic oxides with phosphoric acid at different reaction times. Since then, different types of metal phosphates were synthesized based on acid–base reaction approach. The formation can be sum up briefly with three steps: (i) dissolution of oxides in an acid phosphate solution, (ii) ion formation and reaction (iii) saturated gel–crystallization formation [22, 23].

During the dissolution mechanism of oxides in acid solution, pH was important. Dissolution of phosphoric acid and metal oxide were given in Eqs. (1) and (2):

$$H_3PO_4 \rightarrow mH^+ + H_{3-m}PO_4^{m-} \quad (m = 0\text{–}3), \qquad (1)$$

$$MO_n + 2nH^+ \rightarrow M_{(aq)}^{2n+} + nH_2O. \qquad (2)$$

As it was seen from Eqs. (1) and (2), dissolution increased with higher pH values. After the dissolution of starting materials at determined conditions, the hydrophosphate formation has occurred. Hydrothermal conditions are generally used for the phosphate

Table 1. Crystallographic data of the synthesized magnesium phosphate phases

Sample code	Phase A	Phase B
Pdf code	01-075-1714	00-044-0775
Mineral name	Newberyite	Magnesium phosphate hydrate
Mineral formula	$MgHPO_4 \cdot 3H_2O$	$Mg_3(PO_4)_2 \cdot 22H_2O$
Crystal system	Orthorhombic	Triclinic
a, *b*, *c,* Å	10.20, 10.68, 10.01	6.93, 6.93, 16.15
[α, β, γ], deg	[90.0, 90.0, 90.0]	[82.2, 89.7, 119.5]

synthesis. The characteristic features are notable for the applications. The gelling of the magnesium phosphate is required the long reaction times and the suitable organic/inorganic additives [6, 7, 18].

The morphological and structural characteristics of the prepared particles might be controlled by the reaction parameters such as the reagents stoichiometry, the temperature and pH without using any modifying agent. In this study, it is aimed to study the effect of solution alkalinity on the synthesis of magnesium phosphate hydrates. The differences in characteristic properties were determined by the characterization of samples. The samples were identified with XRD and characterized by the spectroscopies of FT-IR and Raman. The morphologies of samples were analysed with SEM. Thermal behaviours of samples were investigated with thermogravimetric analyses.

EXPERIMENTAL

Materials. The magnesium and phosphate sources were magnesium oxide (MgO) and orthophosphoric acid (H_3PO_4), respectively. Sodium hydroxide (NaOH) solution was applied for the pH adjustment. All the reagents were supplied from Merck Chemicals and were employed without any further purification and treatment. Distilled water was used for all synthesis and treatment processes.

Hydrothermal synthesis procedure. For the magnesium phosphate precipitation, basic conditions were preferred [21]. The mole ratio of Mg : P was selected as 3 : 2 and the reaction time was 1 hour. The determined amounts of magnesium (Mg) and phosphate (P) sources were reacted in a liquid medium. Experiments were carried out in a glass reactor at the room temperature. The possible reaction for magnesium phosphate reaction (3):

$$3MgO + 2H_3PO_4 + xH_2O \rightarrow Mg_3(PO_4)_2 + yH_2O. \quad (3)$$

The effects of pH experimented in the range of 7–10. The solution of 0.5 M NaOH solution used for pH adjustment under magnetic stirring. pH adjustment was controlled with the pH meter by using a Hanna Instruments' HI 2211 pH/ORP Meter. The synthesized magnesium phosphate particles were separated by filtration and dried at 40°C. The dried particles were ground for the characterization.

Characterization. The synthesized compounds were identified with the X-ray powder diffraction technique by using a Philips PANalytical XPert Pro X-ray diffractometer at 45 kV, 40 mA and CuK_α radiation in the 2θ range of 5°–60°. The characteristic band values of functional groups in prepared samples were analysed by using the spectroscopic techniques of FT-IR and Raman. A PerkinElmer Spectrum One FT-IR was used for the FT-IR analyses with a sampling accessory of universal attenuation total reflectance (ATR) with a diamond/ZnSe crystal. In the Raman analyses, a Perkin Elmer brand Raman Station 400F was employed. The morphology of surface and particle features of the prepared samples were examined by using a CamScan Apollo 300 field-emission SEM at 15 kV. Thermal behaviour of the samples was investigated by using a Perkin Elmer Diamond TG/DTA. The thermogravimetric analyses were applied between the temperature ranges of 40–500°C, at the heating rate of 10°C/min and an inert (N_2) atmosphere.

RESULTS AND DISCUSSION

X-ray powder diffraction results. X-ray powder diffraction patterns of synthesized magnesium phosphate compounds are presented in Fig. 1. Products were identified as a mixture of magnesium phosphate hydrates. Based on XRD results, the identified phases of magnesium phosphates were coded as Phase A (newberyite ($MgHPO_4 \cdot 3H_2O$) with the pdf no. of 01-075-1714) and Phase B (magnesium phosphate hydrate ($Mg_3(PO_4)_2 \cdot 22H_2O$) with the pdf no. of 00-044-0775). The sample synthesized at pH 7 were identified as Phase A. There was a tendency for the formation of Phase B with the increasing pH values. At the pH values of 8 and 9, the mixtures of Phase A and B were obtained. Pure Phase B were determined at pH 10.

Crystallographic data of the synthesized magnesium phosphate phases are given in Table 1.

For the Phase A, the characteristic peaks [*h k l* ($d_{spacing}$)] of $MgHPO_4 \cdot 3H_2O$ were seen at the 2θ positions of 14.92° [1 1 1 (5.94 Å)], 16.62° [0 2 0 (5.34 Å)], 17.38° [2 0 0 (5.10 Å)], 18.83° [0 2 1 (4.71 Å)], 19.77°

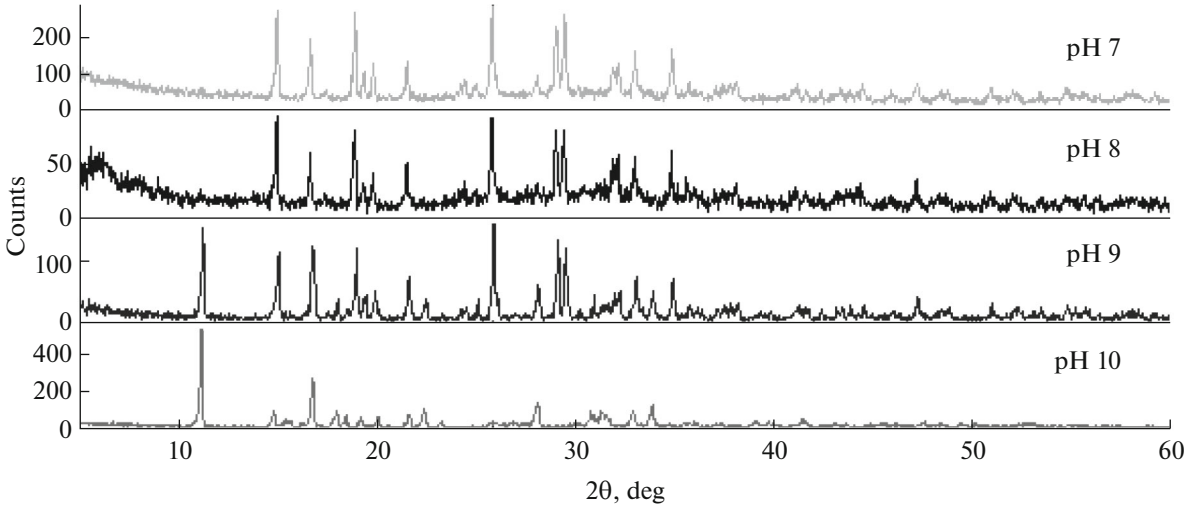

Fig. 1. X-ray powder diffraction pattern of synthesized magnesium phosphate compounds.

[1 0 2 (4.49 Å)], 21.45° [1 1 2 (4.14 Å)], 24.90° [2 0 2 (3.57 Å)], 25.74° [2 2 1 (3.46 Å)], 28.01° [1 3 1 (3.19 Å)], 28.96° [3 1 1 (3.08 Å)], 30.10° [2 2 2 (2.97 Å)], 32.92° [3 1 2 (2.72 Å)], 34.78° [0 4 1 (2.58 Å)], and 35.60° [1 4 1 (2.50 Å)] [24].

For the Phase B, the characteristic peaks [*h k l* ($d_{spacing}$)] of $Mg_3(PO_4)_2 \cdot 22H_2O$ were seen at the 2θ positions of 11.11° [0 0 2 (7.96 Å)], 16.71° [0 0 3 (5.30 Å)], 28.04° [0 0 5 (3.18 Å)], 30.81° [2 0 2 (2.90 Å)], 31.25° [−2 2 2 (2.86 Å)], 32.78° [1 −1 5 (2.73 Å)] and 33.80° [0 0 6 (2.65 Å)] [17].

Spectroscopic results. The characteristic band values of samples were observed in the ranges of 4000–500 cm^{-1} for FT-IR spectroscopy and 3280–250 cm^{-1} for Raman spectroscopy, respectively. FT-IR spectra of synthesized magnesium phosphates are shown in Fig. 2. The characteristic stretching over the 3200 cm^{-1} could be explained with the OH bands in the hydrate structure. Vibrational band of $\nu(PO_2(OH))$ was observed in the range of 3100–2800 cm^{-1}. The peak values between 1700 and 1600 cm^{-1} were assigned to the H–O–H bands. In accordance with X-ray powder diffraction results, the peaks for the H–O–H bands became apparent with the phase formation of $Mg_3(PO_4)_2 \cdot 22H_2O$. The symmetrical stretching of PO_3^- and PO_4^{3-} were seen in the regions of 1200–1100 and 1100–1000 cm^{-1}, respectively. The $PO_2(OH)$ bending was approximately seen at 885 cm^{-1}. The peaks observed at lower than 700 cm^{-1} can be explained with the out of plane of phosphate ions [6, 7, 24].

Raman spectra of synthesized magnesium phosphates are shown in Fig. 3. The characteristic band values for the hydroxyl stretching was seen in the range of 3280–1500 cm^{-1}. There was stronger stretching seen at the higher pH values because of the increase in crystal water bonded to phosphate structure. The symmetric stretching between the P and O atoms can be seen at 1155 cm^{-1}. The strong peak around the 1000 cm^{-1} can be explained with symmetric stretching between P and O atoms. The asymmetric stretching between the phosphate and hydroxyl ions was observed at around 895 cm^{-1}. The out of plane bands were seen in the range of 560–520 cm^{-1}, while in-plane bands were seen at lower the band values of 410 cm^{-1} [26].

SEM results. SEM morphologies of synthesized magnesium phosphates are presented in Fig. 4. The synthesized particle sizes were in micro-scale. In accordance with the X-ray powder diffraction results, the differences were observed in surface morphologies with the increasing pH value. At pH 7, flowerlike particles were obtained in the range of 1.17–2.04 μm. With increasing pH to 8, flowerlike particles turned unshapely and nebulously particles. The particle sizes were between 1.94–2.56 μm. As the pH increased, particle shapes were transformed into flat layers and particle sizes were increased. The largest particles (in the range 3.16–9.85 μm) were obtained at pH 10 and particle's shapes can be explained by the formation of nested flat sheets.

Thermogravimetric results. Under heating treatment, the removal of structural water from the compound is called dehydration [27–29]. Thermal dehydration behaviours of samples prepared at different pH values were examined with thermal analyses techniques. Thermal curves of samples were presented in Fig. 5. As it is seen at TG-DTG curves from Fig. 5, the dehydration process of synthesized magnesium phosphates was observed in the temperature range of 40 and 250°C. As it is seen from the thermogram of phases A and B, two different thermal behavior were

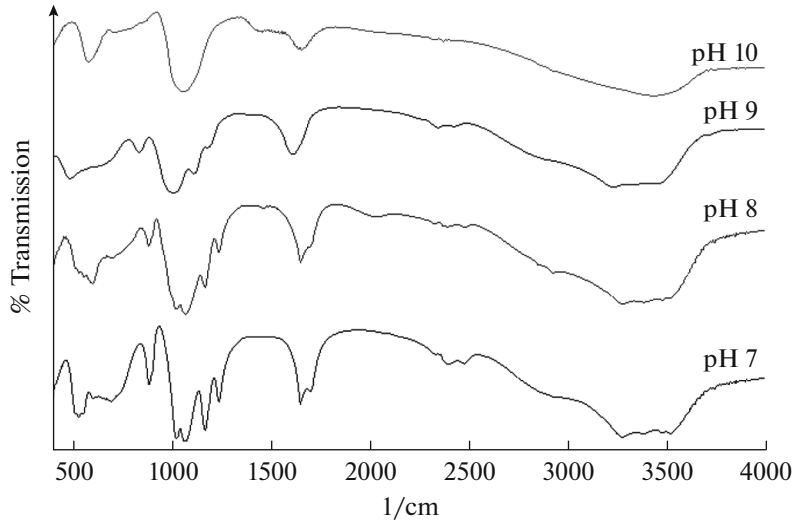

Fig. 2. FT-IR spectra of synthesized magnesium phosphate compounds.

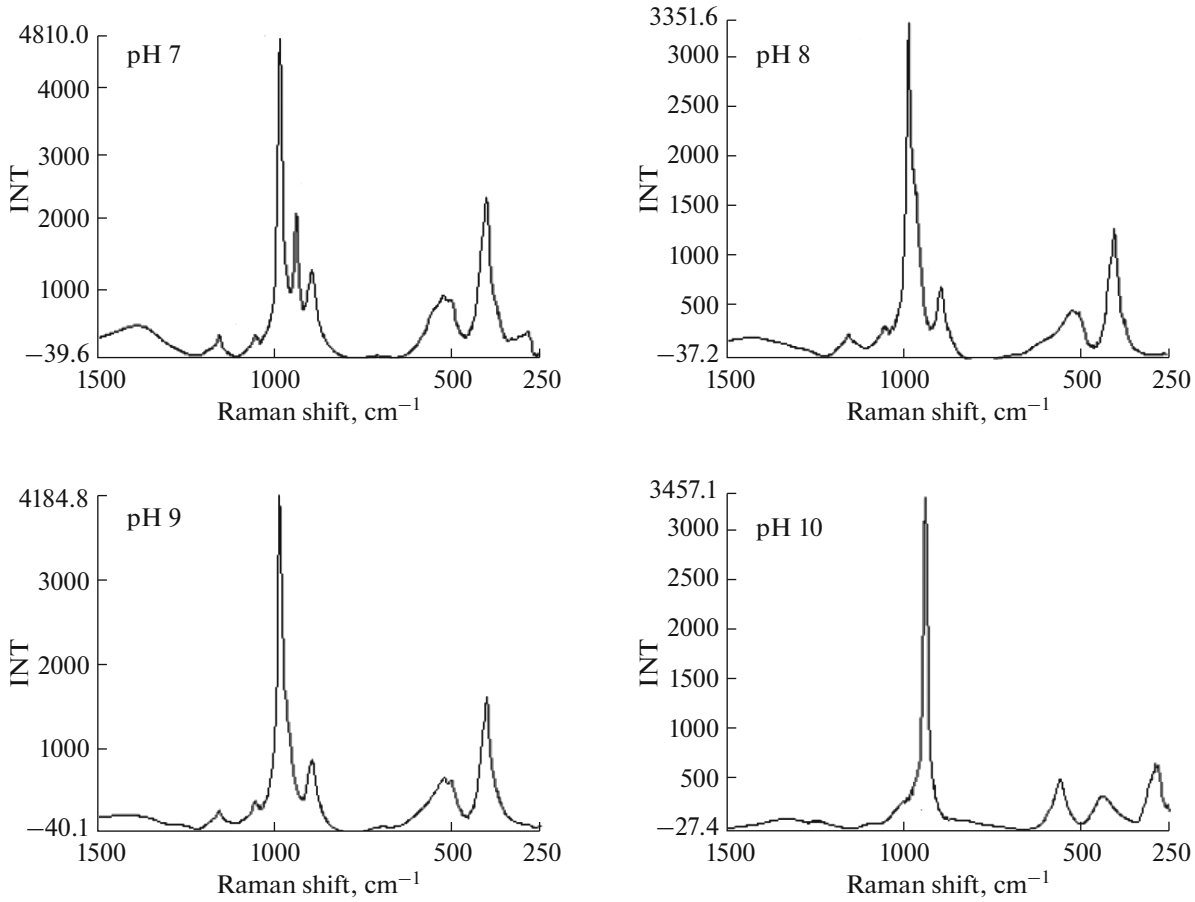

Fig. 3. Raman spectra of synthesized magnesium phosphate compounds.

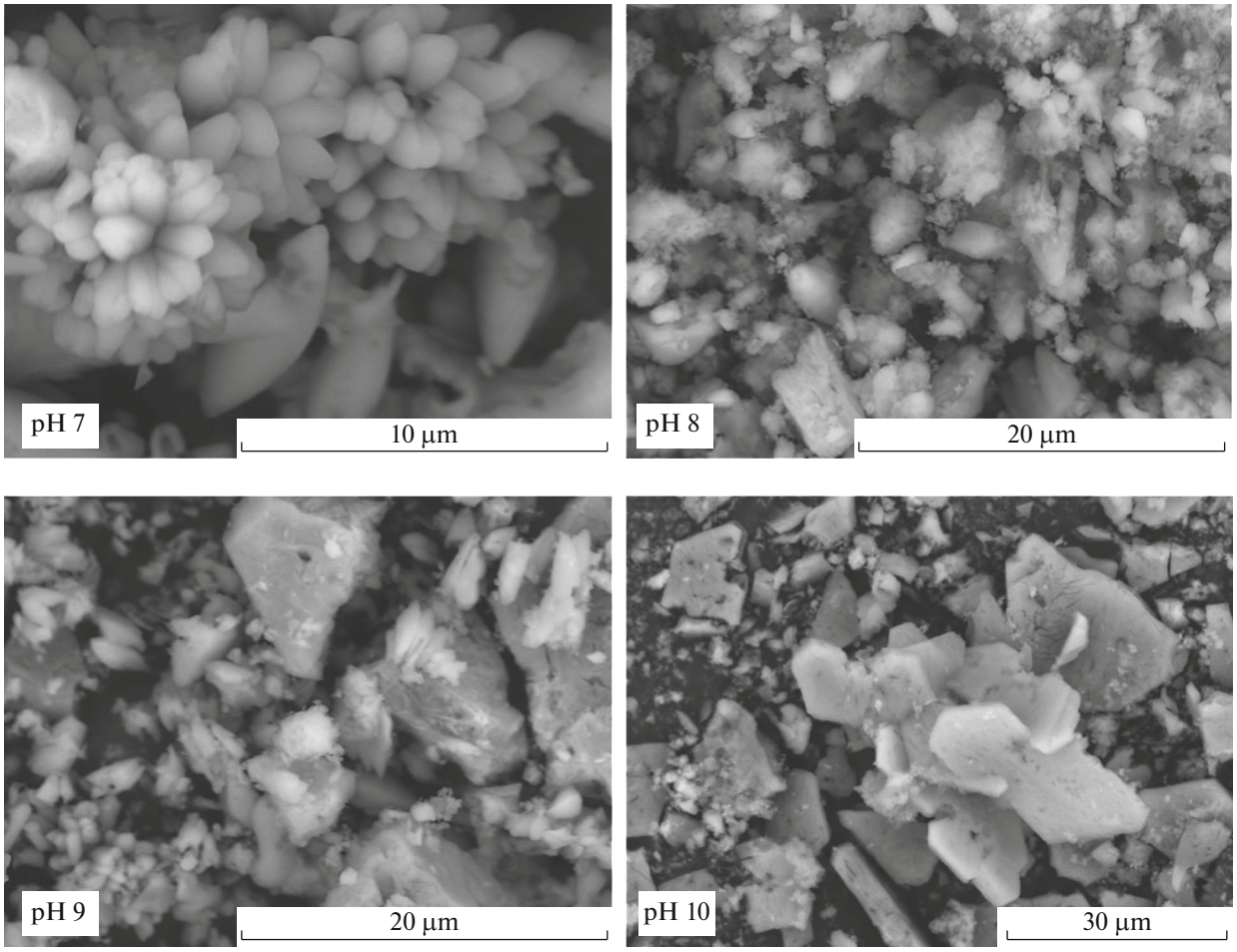

Fig. 4. SEM morphologies of synthesized magnesium phosphates.

seen. Thermogravimetric results of samples are given in Table 2.

These two different thermal behaviours were seen with the formation of two different phases. In phase A, dehydration behaviour can be explained by a two-step reaction. The first step was seen in the range of 67.66–109.22°C and the peak of the DTG curve were determined at 94.95°C. The average weight loss was 12.70% for the first step, equal to a value of 1.21 mole of water. The second step occurred in the range of 109.22–189.96°C and the peak of the DTG curve were observed at 128.95°C. The average weight loss was 18.80% for the first step, equal to a value of 1.79 moles of water. In phase B, dehydration behaviour can be explained by a single step reaction. The dehydration of the compound was seen in the range of 39.95–180.29°C and the peak of the DTG curve were determined at 74.34°C. The average weight loss was deter-

Table 2. Thermal analyses results of synthesized samples at different pH values

Sample	Step	T_i, °C	T_f, °C	$T_{p(DTG)}$, °C	Total mass loss, %
pH 7	1st	67.66	109.22	94.95	31.5
	2nd	109.22	189.96	128.95	
pH 8	1st	48.94	73.29	60.93	32.9
	2nd	106.99	198.96	139.05	
pH 9	1st	41.46	96.93	72.19	39.0
	2nd	106.55	189.20	130.66	
pH 10	1st	39.95	180.29	74.34	55.5

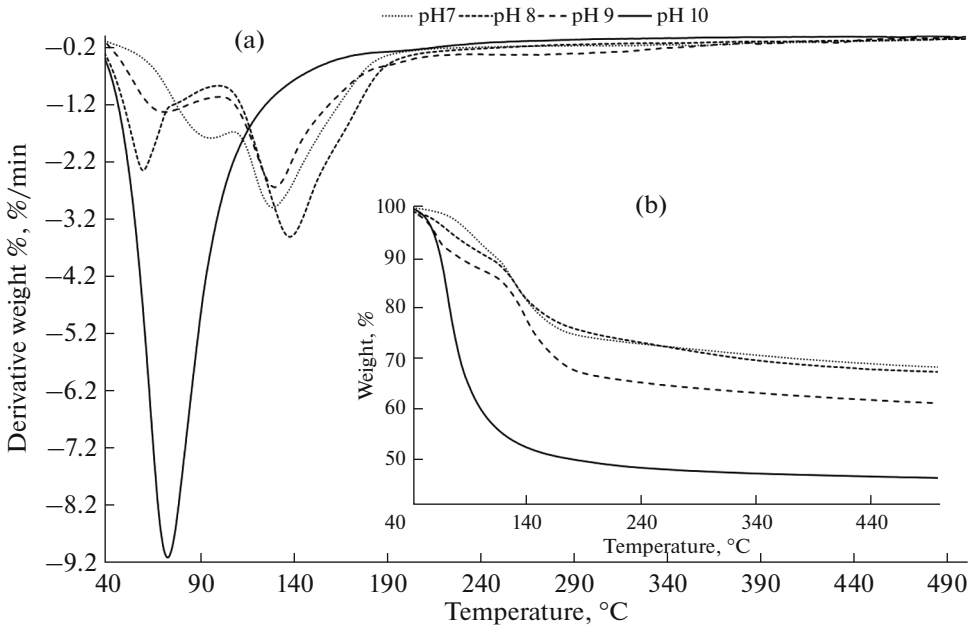

Fig. 5. Thermal curves of synthesized samples at different pH values: (a) DTG and (b) TG.

mined 55.50% for the $Mg_3(PO_4)_2 \cdot 22H_2O$. In accordance with XRD results, the increase in mass losses was determined with the increasing pH values.

CONCLUSIONS

In this paper, two different types of magnesium phosphate hydrates ($MgHPO_4 \cdot 3H_2O$ and $Mg_3(PO_4)_2 \cdot 22H_2O$) were synthesized from magnesium oxide and phosphoric acid at various pH values. According to the X-ray powder diffraction results, pure $MgHPO_4 \cdot 3H_2O$ and $Mg_3(PO_4)_2 \cdot 22H_2O$ prepared at pH 7 and 10, respectively. The morphologies of synthesized magnesium phosphate hydrates were studied with the SEM analyses. $MgHPO_4 \cdot 3H_2O$ compound had flowerlike particles whereas $Mg_3(PO_4)_2 \cdot 22H_2O$ had agglomerations of layers. Synthesized particles were in micro-scale and with the effect of agglomeration on larger particle sizes were determined at increasing alkalinity. As a conclusion, a tendency of $Mg_3(PO_4)_2 \cdot 22H_2O$ phase formation was observed with the increasing alkalinity. In addition, particle shape and formation can be modified by the controlling of reaction conditions without using any modifying agent.

REFERENCES

1. F. Qiao, C. K. Chau, and Z. Li, Constr. Build. Mater. **24**, 695 (2010). https://doi.org/10.1016/j.conbuildmat.2009.10.039
2. G. Metres and M. P. Ginebra, Acta Biomater. **7**, 1853 (2011). https://doi.org/10.1016/j.actbio.2010.12.008
3. Z. Mesikova, P. Sulcova, and M. Trojan, J. Therm. Anal. Calorim. **88**, 103 (2007). https://doi.org/10.1007/s10973-006-8099-8
4. B. Boonchom, J. Therm. Anal. Calorim. **98**, 863 (2009). https://doi.org/10.1007/s10973-009-0108-2
5. Y. H. Liu, S. Kumar, J. H. Kwag, and C. S. Ra, J. Chem. Technol. Biotechnol. **88**, 181 (2013). https://doi.org/10.1002/jctb.3936
6. M. A. Aramendia, V. Borau, C. Jimenez, et al., J. Colloid. Interf. Sci. **240**, 237 (2001). https://doi.org/10.1006/jcis.2001.7565
7. M. A. Aramendia, V. Borau, C. Jimenez, et al., J. Colloid. Interf. Sci. **219**, 201 (1999). https://doi.org/10.1006/jcis.1999.6472
8. J. A. Kim, H. Yun, Y. Choi, et al., Biomater. **157**, 51 (2018). https://doi.org/10.1016/j.biomaterials.2017.11.032
9. Y. Li, Y. Li, T. Shi and J. Li, Const. Build. Mater. **96**, 346 (2015). https://doi.org/10.1016/j.conbuildmat.2015.08.012
10. A. Bensalem and G. Iyer, J. Solid. State. Chem. **114**, 598 (1995). https://doi.org/10.1006/jssc.1995.1092
11. K. Kongshaug, H. Fjellvag, and K. P. Lillerud, Solid. State. Sci. **3**, 353 (2001). https://doi.org/10.1016/S1293-2558(00)01109-2
12. A. Bensalem, M. Ahluwalia, T. V. Vijayaraghavan, and Y. H. Ko, Mater. Res. Bull. **32**, 1473 (1997). https://doi.org/10.1016/S0025-5408(97)00129-3
13. S. V. Golubev, O. S. Pokrovsky, and V. S. Savenko, J. Cryst. Growth **223**, 550 (2011). https://doi.org/10.1016/S0022-0248(01)00681-9

14. A. Bensalem, G. Iyer, and S. Amar, Mater. Res. Bull. **30**, 1471 (1995). https://doi.org/10.1016/0025-5408(95)00168-9

15. M. Sadiq, M. Bensitel, C. Lamonier, and J. Leglise, Solid. State Sci. **10**, 434 (2008). https://doi.org/10.1016/j.solidstatesciences.2007.12.037

16. G. J. Racz and R. J. Soper, Can. J. SoiI Sci. **48**, 265 (1968). https://doi.org/10.4141/cjss68-036

17. S. N. Britvin, G. Ferraris, G. Ivaldi, et al., N. Jb. Miner. Mh. **4**, 160 (2002). https://doi.org/10.1127/0028-3649/2002/2002-0160

18. T. Kanazawa, T. Umegaki, and M. Shimizu, B: Chem. Soc. Jpn. **52**, 3713 (1979). https://doi.org/10.1016/S1293-2558(00)01109-2

19. H. Assaaoudi, Z. Fang, I. S. Butler, et al., Solid State Sci. **9**, 385 (2007). https://doi.org/10.1016/j.solidstatesciences.2007.03.015

20. H. Zhou, J. F. Luchini, and J. Bhaduri, J. Mater. Sci.: Mater. Med. **23**, 2831 (2012). https://doi.org/10.1007/s10856-012-4743-y

21. S. Mousa, Phosphorus Res. Bull. **24**, 16 (2010). https://doi.org/10.3363/prb.24.16

22. A. S. Wagh and S. Y. Jeong, J. Am. Ceram. Soc. **86**, 1838 (2003). https://doi.org/10.1111/j.1151-2916.2003.tb03569.x

23. J. M. Poplawska, M. Pernechele, T. Troczynski, et al., J. Mol. Struct. **1180**, 215 (2019). https://doi.org/10.1016/j.molstruc.2018.11.087

24. G. R. Sivakumar, *In Vitro Studies on the Growth and Characterization of the Crystalline Constituents of Metabolic Acid and Nonmetabollic Urinary Stones: Dicalcium Phosphate and Magnesium Phosphate* (Anna University, India, 2000).

25. R. L. Frost, W. Martens, P. A. Williams, and J. T. Kloprogge, Mineral. Mag. **66**, 1063 (2002). https://doi.org/10.1180/0026461026660077

26. R. L. Frost, S. Palmer, and R. E. Pogson, Spectrochim. Acta A **79**, 1149 (2011). https://doi.org/10.1016/j.saa.2011.04.035

27. F. T. Senberber, Main Group Chem. **16**, 151 (2018). https://doi.org/10.3233/MGC-170233

28. M. A. Kremennaya, A. P. Budnyk, M. A. Soldatov, et al., J. Struct. Chem. **59**, 64 (2018). https://doi.org/10.1134/S0022476618010109

29. N. N. Golovneva, M. S. Molokeeva, and I. V. Sterkhovad, Russ. J. Inorg. Chem. **64**, 1146 (2019). https://doi.org/10.1134/S0036023619090134